Available online at www.sciencedirect.com
SCIENCE DIRECT
Journal of Molecular Catalysis A: Chemical 241 (2005) 79–87
JOURNAL OF MOLECULAR CATALYSIS A: CHEMICAL
www.elsevier.com/locate/molcata

Synthesis, characterization and catalytic activity of Mn(III)- and Co(II)-salen complexes immobilized mesoporous alumina

V.D. Chaube, S. Shylesh, A.P. Singh *

Inorganic and Catalysis Division, National Chemical Laboratory, Pune 411008, India

Received 6 May 2005; received in revised form 24 June 2005; accepted 1 July 2005
Available online 10 August 2005

Abstract

Mn(III) and Co(II)–schiff base complexes were immobilized over mesoporous alumina through the reaction of mesoporous alumina functionalized 3-aminopropyl triethoxy silane (3-APTES) and salicylic aldehyde via schiff base condensation. The surface properties of the functionalized catalysts were analyzed by a series of characterization techniques like elemental analysis, PXRD, FTIR, N_2 adsorption–desorption, TG-DTG, DR UV–vis, XPS, etc. PXRD and adsorption–desorption analysis shows that the mesostructure of alumina remains intact after various modifications, while spectral technique show the successful anchoring of the neat complexes inside the porous alumina support. The catalytic activity of the functionalized metal-salen complexes examined in the liquid phase oxidation of styrene and cyclohexene shows that the functionalized salen complexes are more active and selective than the corresponding neat metal complexes. Further, the catalyst (Mn-S-NH_2-MA) was recycled three times in the oxidation of styrene and no major change in the conversion and selectivity is observed, which shows that the immobilized metal-salen complexes are stable under the present reaction conditions.

Keywords: Mesoporous alumina; Immobilization; Schiff base complexes; Oxidation

1. Introduction

After the discovery of silica based ordered mesoporous materials of M41S family by Mobil researchers [1], much attention had been focused in the synthesis of non-siliceous mesoporous materials due to its potential applications in the field of separation science, nano science, catalysis, etc. Huo et al. [2] and Sayari and Liu [3] demonstrated the synthesis of a variety of non-siliceous mesoporous materials, among them, only a few exhibit better stability and increased mesostructural ordering after the removal of the structure directors which limits its use as a catalyst or catalyst support. Hence, the synthesis of non-siliceous mesoporous materials with better stability remains a challenge because compared to its oxide form, the mesoporous materials possess high surface areas and variable pore sizes and hence can be finely tuned for specific applications like selective adsorption process by the suitable anchoring of various organic pendant groups [4]. Thus, the synthesis of various organic–inorganic hybrid mesoporous materials emerges as a potential tool to anchor various homogenous metal salts/complexes and it is interesting to probe the stability of such materials during various modification processes.

Heterogenization of homogenous catalysts has been an interesting area of research in an academic and in an industrial point of view, as this method can provide an ideal way for combining the advantages of homogenous catalysts and simultaneously avoiding its disadvantages like handling and reusability [5,6]. Mn/Co (salen) complexes have been reported as efficient catalysts for the epoxidation of various olefins [7–9]. The increasing interest towards this reaction brought some authors to develop the heterogenous form of Mn(III)/Co(II)-salen catalysts and to date, three kinds of approaches have been generally adopted [10–16]. First, Mn-salen complexes were supported on polymers for a better reusability of the materials. For instance, Janssen et al. [17] have synthesized a dimeric form of (salen) Mn(III) ligand

* Corresponding author. Tel.: +91 20 2589 3761; fax: +91 20 2589 3761.
E-mail address: apsingh@cata.ncl.res.in (A.P. Singh).

1381-1169/$ – see front matter © 2005 Elsevier B.V. All rights reserved.
doi:10.1016/j.molcata.2005.07.005

and retained this complex in the cross-linked polymer membrane and used as a catalyst for epoxidation reactions, while Mintolo et al. [18] synthesized the polymer-bound salen Mn(III) complex by copolymerization of salen complex with styrene and divinylbenzene. Secondly, the encapsulation of salen complex was performed by using the so-called, 'ship in a bottle' technique. Sabater et al. [19] synthesized Mn(III)-salen complex of simple structure inside the supercage of Y-zeolites and showed that the catalytic activity was similar to that of chloride complexes in the homogenous phase. Alternatively, Mn(III)-salen ligands were immobilized by an ion exchange mechanism like the embedding of selective homogenous Mn(III) cationic salen complexes into the pores of mesoporous MCM-41 materials [20]. Hence, novel routes for the anchoring of these metal complexes over various supports having good stability and open channels rely as a potential way to extend their applicability and reusability.

The present work deals with the synthesis and characterization of metal (salen) complexes immobilized mesoporous alumina, performed by the chemical anchoring of the complex to the support surface via suitable modifications. The heterogenity of the developed materials were verified in the epoxidation reaction of various olefins and the performance was compared with the homogenous counterparts. To the best of our knowledge, this is the first report detailing the immobilization of salen-ligated metals via condensation procedure over mesoporous alumina.

2. Experimental

2.1. Synthesis

The materials used for the synthesis were aluminium isopropoxide (Aldrich), lauric acid (Loba Chemie), 1-propanol (Merck), 3-aminopropyl triethoxy silane (3-APTES, Lancaster), salicyl aldehyde (Merck), cobalt(II) acetate and manganese(III) acetate (Aldrich).

2.1.1. Preparation of mesoporous alumina (MA)

Non-siliceous mesoporous alumina was synthesized according to the following procedure at a temperature of 110 °C using carboxylic acid (lauric acid) as surfactant [21]. The composition of gel mixture; Al-isopropoxide:lauric acid:1-propanol is 1:0.03:26. Typically, an aluminum hydroxide suspension was prepared by the hydrolysis of 43.8 g of Al-isopropoxide with 10.3 g of deionised water in 275 g of 1-propanol (99%). After stirring for 1 h, 10.8 g of lauric acid (99.5%) was added slowly to the gel mixture. The mixture was aged for 24 h at room temperature and then heated under static conditions at 110 °C in a glass jar for 2 days. The solid material obtained was then filtered, washed with ethanol and dried at 100 °C for 4–5 h. Finally, the material was calcined at a temperature of 450 °C with a temperature ramp of 1 °C/min from room temperature to the final temperature. The calcination atmosphere was nitrogen during the earlier stages (<200 °C) and air at final temperatures.

2.1.2. Preparation of 3-APTES functionalized mesoporous alumina (NH_2-MA)

To a suspension of 10 g of calcined mesoporous alumina in 50 ml dry toluene, 2.68 g of 3-aminopropyl triethoxy silane was added slowly and heated to reflux with continuous stirring for 8 h under nitrogen atmospheres (Scheme 1). The powdery sample containing amino groups was filtered, washed with acetone and then soxhlet extracted using a solution mixture of diethyl ether and dichloromethane (1:1) for 24 h and dried under vacuum. Elemental analysis shows that 0.89% of nitrogen gets introduced into the mesoporous support, which indicates that ~52% of 3-APTES was immobilized per gram of mesoporous alumina.

2.1.3. Preparation of neat Co(II) and Mn(III) complexes

Cobalt and manganese (salen) precursors were prepared according to the following procedure. The appropriate metal (cobalt and manganese) acetate hydrate (6.0 mmol) in ethanol (10 ml) was added slowly to a solution of salicyl aldehyde (2.94 g, 24.0 mmol) in ethanol (40 ml). The solutions were stirred at room temperature for 24 h and their subsequent concentration leads to precipitation of the corresponding metal (salen) precursor (Scheme 2). The solid product obtained was washed with copious amounts of chloroform and dried in vacuum at 100 °C for 24 h. Elemental analysis data obtained after purification are as follows; theoretical value (actual value) of C (%) 56.56 (58.18), H (%) 3.36 (4.11) for Mn complex, while Co complex shows C (%) 58.18 (56.49) and H (%) 3.32 (3.01).

2.1.4. Preparation of salen Co(II) and salen Mn(III) complexes immobilized on modified mesoporous alumina (Co/Mn-S-NH_2-MA).

The synthesized neat complex, viz. (bis-salicyl aldehyde) M, has been chemically anchored to the aminopropyl-modified alumina support, using a procedure as shown in Scheme 3 [22]. The material was then soxhlet extracted, using

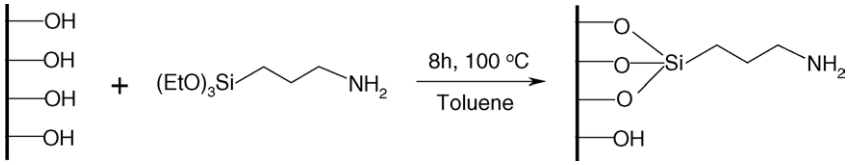

Scheme 1.

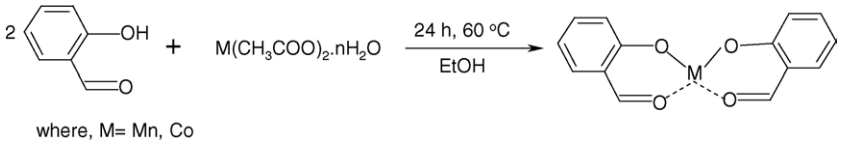

Scheme 2.

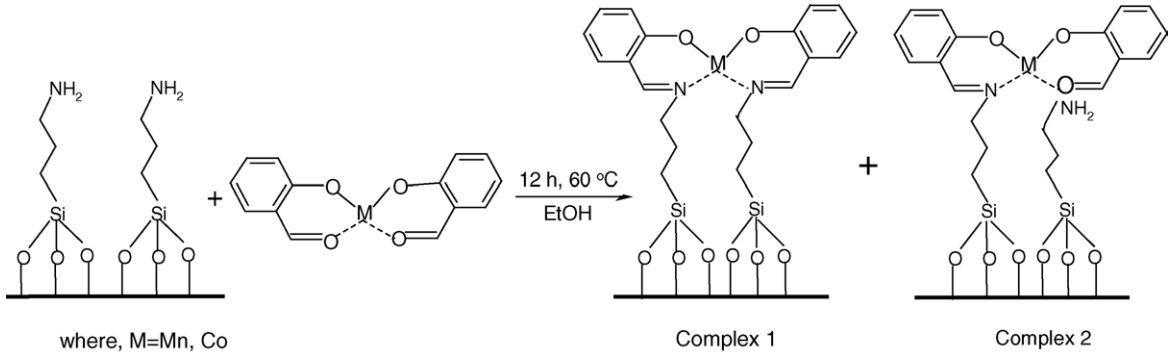

Scheme 3.

a mixture of $CHCl_3$–EtOH mixture for 12 h to remove the unreacted organic residue from the mixture.

2.2. Characterization

Analysis of the organic material incorporated on the solid mesoporous material was carried out by using EA1108 Elemental Analyzer (Carlo Erba Instruments). X-ray diffraction measurements were carried out on a Rigaku Miniflex diffractometer using Cu Kα radiation at a scan rate of 3°/min from 1.5° to 50°. FTIR spectra of the solid samples were taken in the range of 4000–400 cm^{-1} on a Shimadzu FTIR 8201 instrument by diffuse reflectance scanning disc technique. The specific surface area, total pore volume and average pore diameter were measured by N_2 adsorption–desorption method using NOVA 1200 (Quanta chrome). The samples were activated at 200 °C for 3 h under vacuum and then the adsorption–desorption was conducted by passing nitrogen into the sample, which was kept under liquid nitrogen. Pore size distribution (PSD) was obtained by applying the BJH pore analysis applied to the adsorption branch of the nitrogen adsorption–desorption isotherm. Thermogravimetric and differential thermogravimetric (TG-DTA) analysis of the neat and immobilized Co-salen complexes and Mn-salen complexes was recorded on a Rheometric Scientific (STA 1500) analyzer. Diffuse reflectance UV–vis spectra were recorded in the range 200–600 nm with a Shimadzu UV-2101 PC spectrometer equipped with a diffuse reflectance attachment, using $BaSO_4$ as reference. XPS spectra were recorded on a VG micortech multilab-ESCA 3000 spectrometer equipped with a twin anode of Al and Mg. All the measurements are made on powder samples using Mg Kα X-ray at room temperature. Base pressure in the analysis chamber was 4×10^{-10} Torr. The overall energy resolution of the instrument is better than 0.7 eV, determined from the full width at half maximum of the $4f_{7/2}$ core level of the gold surface. The error in all the binding energy (BE) values was within ±0.1 eV. The correction in binding energy was performed by using the C1s peak of carbon at 284.9 eV, as reference.

2.3. Catalytic measurements

In a typical reaction, TBHP (0.45 g, 5 mmol) was added to a solution of styrene (0.52 g, 5 mmol) in acetonitrile (6 g) containing 0.2 g of catalyst (pre-activated at 100 °C for 2 h). The reaction mixture was magnetically stirred at 60 °C in a silicone oil bath. Samples of the reaction mixture were taken periodically and analyzed by gas-chromatograph (HP 6890) equipped with a flame ionization detector (FID) and a capillary column (5 μm thick cross-linked methyl silicone gum, 0.2 m × 50 m). The products were further identified by GC-MS analysis (Shimadzu 2000 A).

3. Results and discussion

Fig. 1 depicts the XRD patterns of as-synthesized, calcined, aminopropyl-modified and complex functionalized mesoporous alumina. The diffraction patterns of as-synthesized and calcined forms of mesoporous alumina shows a broad reflection at a 2θ value of 2.6, assigned to the (1 0 0) reflection of the hexagonal lattice. Even though the XRD patterns are devoid from any higher order reflections, the intensity of the characteristic d_{100} peak of calcined mesoporous alumina is quite pronounced and is similar to earlier reports over non-siliceous mesoporous materials [23,24]. The absence of higher order reflections indicates that the pore walls are amorphous or there is a lack of correlation between the structures of adjacent pores. Further, after mod-

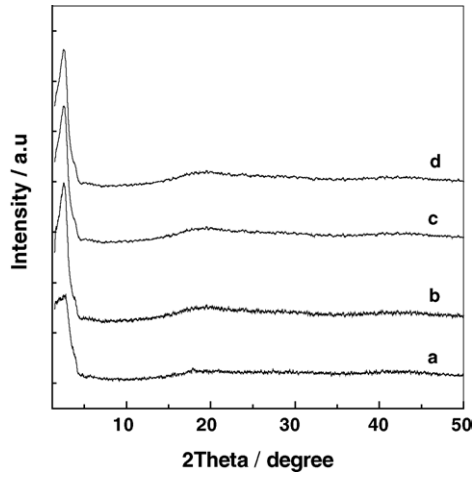

Fig. 1. XRD patterns of: (a) as-synthesized mesoporous alumina; (b) calcined mesoporous alumina; (c) aminopropyl-modified mesoporous alumina; (d) Co-salen immobilized mesoporous alumina.

ifications, the intensity of the characteristic d_{100} reflection gets decreased while the mesostructure remains intact. These results show that the anchoring of the functionalized moieties (3-APTES and further anchoring of salen complexes), inside the pore channels of mesoporous alumina, had not damaged the overall structure of the support material.

The IR spectra of as-synthesized, calcined, 3-APTES-modified and Co(II)- and Mn(III)-salen immobilized mesoporous alumina in the 4000–400 cm^{-1} range are presented in Fig. 2A and B. The as-synthesized samples exhibit bands at 2930 and 2870 cm^{-1} corresponding to C–H vibrations of the surfactant molecules, but in the case of calcined samples, the peaks disappeared due to removal of the template molecules. In detail, the spectra of calcined alumina show peaks in the range of 3600–3200 cm^{-1}, attributed to the hydroxyl stretching of the hydrogen bonded internal alumina groups. However, after amine functionalization, new bands appeared at 2939 and 2879 cm^{-1} which are assigned to the asymmetric and symmetric stretching vibrations of $-CH_2$ groups and thus the presence of these bands on NH_2-MA sample shows that amino propyl groups get anchored on the inner wall surface of mesoporous alumina [25,26]. Further, the presence of band at 3300 cm^{-1} in the NH_2-MA sample, assigned to the N–H stretching vibrations of the propyl amino groups, confirms the successful functionalization of 3-APTES groups on the alumina surface (Fig. 2C). After complex immobilization, the band due to N–H vibration gets disappeared with the formation of a new band at 1630 cm^{-1}, which is the characteristic stretching vibration of C=N band [27,28]. These two results clearly indicate the anchoring of Co and Mn complexes over the amino groups of modified mesoporous alumina surface, as shown in Scheme 3. Further, the immobilized complex materials show the characteristic peaks of the neat complexes and thereby confirm that the complex species gets anchored on the pendant organic groups of the mesoporous support.

It is well known that the introduction of homogenous catalysts or metals on porous supports shows a decrease in its specific surface area and pore volume. The support, mesoporous alumina, shows a high surface area of 450 $m^2\,g^{-1}$ and pore volume of 0.4212 ccg^{-1}; after metal complex functionalization, the surface area gets reduced to 223 $m^2\,g^{-1}$ for Co-S-NH_2-MA and 234 $m^2\,g^{-1}$ for Mn-S-NH_2-MA. Thus, the decrease in mesoporous volume (∼52%) and surface area (∼48%) after metal immobilization is indicative of the grafting of complex inside the channels of mesoporous alumina and a detailed list of surface area, pore volume and pore diameter of support and modified samples are given in Table 1. It is clear from table that even though silylation procedures changed the textural properties of the mesoporous

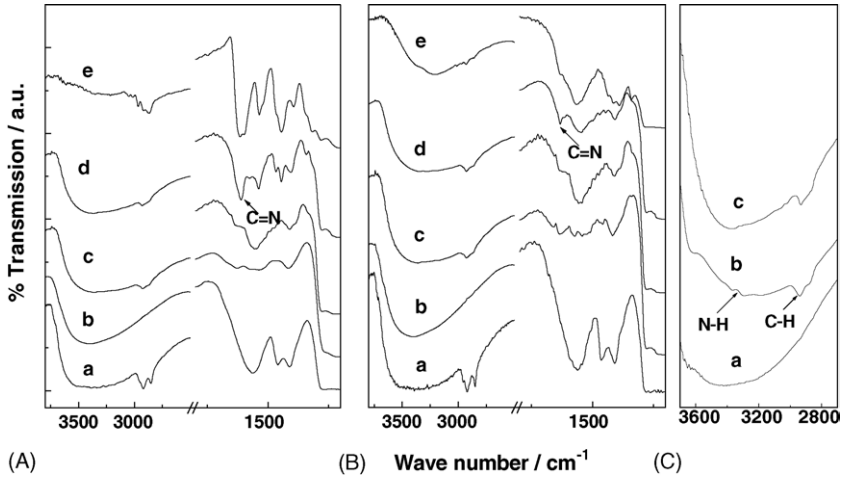

Fig. 2. FTIR spectra of: (A) Co-salen containing mesoporous alumina and (B) Mn-salen containing mesoporous alumina, where (a) as-synthesized mesoporous alumina; (b) calcined mesoporous alumina; (c) aminopropyl-modified mesoporous alumina; (d) metal-salen immobilized mesoporous alumina; (e) neat metal complex, while (C) shows the zoom over 2700–3700 cm^{-1} region of: (a) calcined mesoporous alumina; (b) aminopropyl-modified mesoporous alumina; (c) metal-salen immobilized mesoporous alumina.

Table 1
Textural properties of mesoporous alumina and functionalized samples

Sample	d_{100} (nm)	S_{BET} ($m^2\ g^{-1}$)	Pore volume ($ml\ g^{-1}$)	Pore diameter (nm)
MA	3.17	450	0.4212	4.43
NH_2-MA	3.23	359	0.2311	n.d.
Mn-S-NH_2-MA	3.20	234	0.1821	3.76
Co-S-NH_2-MA	3.33	223	0.1710	3.89

n.d., not determined.

material, the decrease is more prominent after complex immobilization and are due to the presence of bulkier organic moieties inside the pore channel of the support. These results reveal that the anchoring of complex groups had occurred inside the pore channels of mesoporous alumina. Further the adsorption–desorption isotherms of mesoporous alumina and metal complex immobilized mesoporous alumina are of Type IV, according to the IUPAC classification and its steep condensation behaviour indicates the existence of uniformly sized mesopores (Fig. 3). In detail, the alumina support shows an inflection in the $P/P_o \sim 0.5$ range, while after complex immobilization, the P/P_o value changed to a lower value of ~0.45, indicative of some sort of structural damage to the material after modifications and are consistent with the XRD results. Moreover, the BJH pore size distribution analysis shows that the material posses uniformly sized mesopores (see inset of Fig. 3) centered at ca. ~44 Å (Fig. 3A) for alumina support and ca. ~38 Å (Fig. 3B) for the metal complex functionalized samples.

Thermal analysis had been used to monitor the decomposition profiles of the neat as well as anchored metal complexes and the results obtained are depicted in Fig. 4. As-synthesized mesoporous alumina shows two steps of weight loss, when heated under airflow, one at ~100 °C and the other at ~400 °C. The former weight loss is usually attributed to the loss of physisorbed water molecules, while the latter loss attributes to the decomposition of template molecules from the pore channels. A complete decomposition of the surfactant groups below 400 °C indicates that the calcination procedure opted for the removal of structure directors was optimum (see Section 2). In accordance with that, the DTG spectrum of calcined alumina shows only a sharp weight loss below ~100 °C, without any weight losses at higher temperature regions. On the contrary, the TG/DTG spectrum of NH_2-MA shows two steps of weight loss, one below ~100 °C and the other in the region of 340–380 °C. As mentioned, the former weight loss is due to the desorption of physisorbed water, while the second weight loss is attributed to the loss of organo propyl amino fragments [26]. The DTA results further confirm the above results that a strong exothermic peak is observed around ~360 °C for the decomposition of the propyl groups from the alumina surface. The decomposition profiles of homogenous metal complexes get completed at ~468 and ~423 °C for Co- and Mn-salen complexes, respectively, with the residues amounting to cobalt and manganese oxides. Interestingly, after immobilization, the final decomposition temperatures gets increased up to ~626 and ~619 °C for Co-S-NH_2-MA and Mn-S-NH_2-MA complexes, respectively, due to the mutual stabilization of propyl amino groups and the complexes and are indirect proofs for the entrapment of complex moieties inside the pore channels of mesoporous alumina [29].

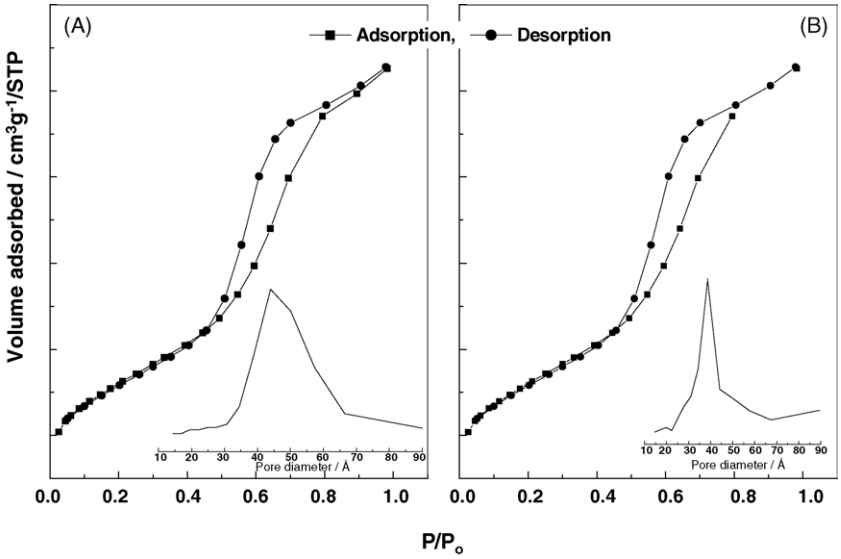

Fig. 3. N_2 adsorption–desorption isotherms and pore size distributions (inset) of: (A) calcined mesoporous alumina and (B) Co-salen immobilized mesoporous alumina.

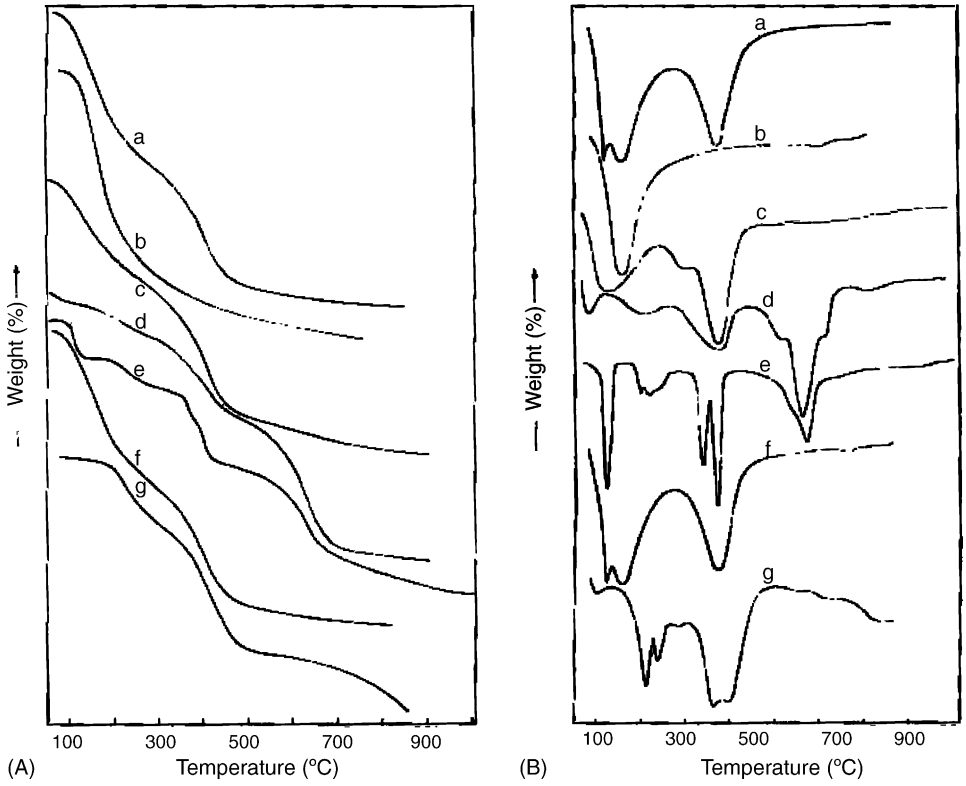

Fig. 4. Thermogravimetric (A) and differential thermogravimetric (B) results of (a) as-synthesized mesoporous alumina; (b) calcined mesoporous alumina; (c) aminopropyl-modified alumina; (d) Mn immobilized mesoporous alumina; (e) Co immobilized mesoporous alumina; (f) neat Mn complex; (g) neat Co complex.

The UV–vis electronic spectra of mesoporous alumina (MA), 3-APTES-modified mesoporous alumina (NH_2-MA), Co(II)/Mn(III)-salen immobilized mesoporous alumina (Co-S-NH_2-MA and Mn-S-NH_2-MA) and homogenous adducts were presented in Fig. 5A and B. The UV–vis spectra of neat Co complex exhibits two broad bands at ∼280 and ∼390 nm, while Mn complex exhibits a broad band at ∼415 nm ascribed to the ligand to metal charge transfer transition bands, akin to related metal (salen) compounds described in the literature [29–31]. After immobilization, for Co (salen) sample, the two distinct bands observed in the neat complex gets overlapped to form a broad band centered around ∼425 nm, whereas for Mn (salen) sample, the spectrum exhibits multiple bands at ∼280, ∼320 and ∼430 nm. Even though a proper

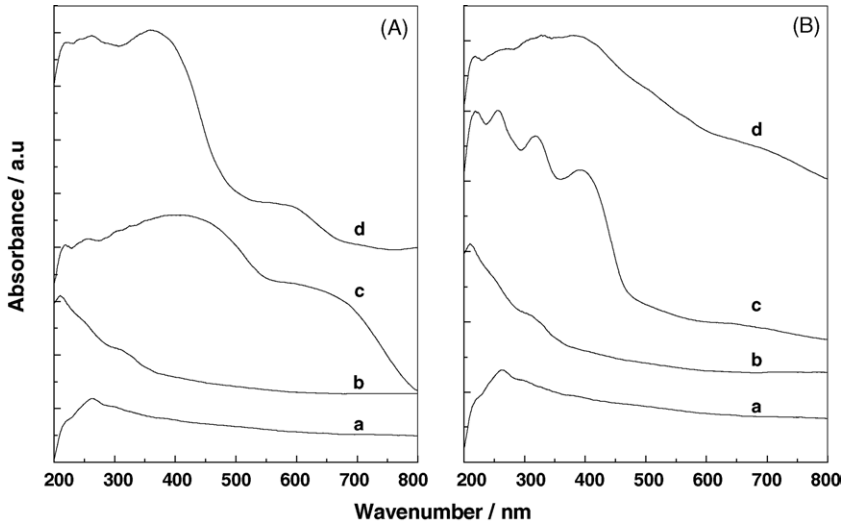

Fig. 5. DR UV–vis spectra of: (A) Co-salen containing mesoporous alumina and (B) Mn-salen containing mesoporous alumina, where (a) calcined mesoporous alumina; (b) aminopropyl-modified mesoporous alumina; (c) metal-salen immobilized mesoporous alumina; (d) neat metal complex.

comparison between the neat and immobilized complex is inappropriate, due to the different coordination spheres, as an indirect evidence it can be concluded that the occurrence of the band at higher wave numbers and its splitting may be due to the different environment and donor sites of the heterogenized metal complexes than the neat complexes. These results are complementary to the data obtained from IR spectra that the immobilization of Co(II)/Mn(III) complexes occurred through schiff base condensation with the amino propyl groups.

X-ray photoelectron spectroscopy (XPS) is a powerful technique used to investigate the electronic properties of the species formed on the surface. As the electronic environment, e.g. oxidation state and/or spin multiplicity influences the binding energy of the core electrons of the metal, XPS is extensively used to attain detailed information about the state of metal species on the surfaces. Fig. 6A and B shows the XPS spectra obtained for pure homogenous adduct and Co(II)- and Mn(III)-salen immobilized mesoporous alumina. Briggs and Seah [32] proposed that the intensity ratio and the energy difference between the two signals obtained for electron ejected from the $p^{1/2}$ and $p^{3/2}$ levels can be used as a tool to investigate the spin multiplicity and therefore to the electronic properties of the cobalt and manganese compounds [33]. The neat manganese complex exhibits Mn $2p_{3/2}$ core level peak at a binding energy of ∼642.5 eV, while the immobilized Mn-salen complex shows a binding energy at ∼643.3 eV and are in accordance with earlier literature data [34]. The observed increased chemical shift of ∼1 eV for the immobilized salen complex than the neat complex attributes to the differences in the coordination environment of metal inside the confined pore channels of mesoporous alumina than under neat conditions. Similarly, cobalt complex also shows an experimental trend as in Mn complexes and matches well with the reported binding energy values of Co $2p_{3/2}$ peak, viz. 779.1 eV for neat cobalt complex and 779.9 eV for immobilized Co-salen complex [35].

3.1. Catalytic reactions

Structural characterization results show that the metal complex is firmly held inside the pore channels of mesoporous alumina and hence the present materials are applied in the liquid phase epoxidation reaction of styrene and cyclohexene. The results obtained from the epoxidation reaction of neat as well as immobilized complexes are presented in Tables 2 and 3 and the kinetic profiles for the activity of neat and immobilized complexes under both reactions are further shown in Fig. 7. From Table 2 and Fig. 7, it is clear that mesoporous alumina functionalized metal complexes show an enhanced activity (calculated in terms of turn over number, TON) and selectivity towards the desired epoxide product than the neat metal complexes. Since the support alumina had a high surface area and moderate pore size, we believe that the confined environment of the metal complex avoids undesirable side reactions like the over oxidation process, as

Table 2
Oxidation of styrene by neat and immobilized metal-salen catalysts

Catalyst	*M* (%)[a]	Conversion (%)	Selectivity (%)			TON[d]
			Epoxide	Benz.[b]	Others[c]	
MA	–	6.3	3.9	95.2	0.87	–
Neat Mn (salen)	0.69	29.5	11.8	79	9.2	22.4
Mn-S-NH_2-MA	0.57	51.4	27.2	70.9	1.9	47.6
Neat Co (salen)	0.87	38.4	9.8	71.6	18.6	24.6
Co-S-NH_2-MA	0.63	55.3	28.2	67.9	3.9	50.0

Reaction conditions: styrene, 0.52 g; TBHP (70%), 0.45 g; CH_3CN, 6 g; T, 60 °C; t, 12 h; catalyst amount, 0.2 g.
[a] *M*, metal content determined from ICP analysis.
[b] Benz., benzaldehyde.
[c] Others, mainly phenyl acetaldehyde and benzoic acid.
[d] TON, turn over number, moles of substrate converted per mole of metal.

Table 3
Oxidation of cyclohexene by neat and immobilized metal-salen catalysts

Catalyst	*M* (%)[a]	Conversion (%)	Selectivity (%)			TON[c]
			Epoxide	One[b]	Others	
MA	–	5.7	12.6	47.1	40.3	25.2
Neat Mn (salen)	0.69	26.7	13.5	70.5	16	25.2
Mn-S-NH_2-MA	0.57	48.5	19.5	69.8	10.7	56.8
Neat Co (salen)	0.87	40.4	20.2	65.2	14.6	33.0
Co-S-NH_2-MA	0.63	56.3	27.6	58.8	13.6	63.3

Reaction conditions: cyclohexene, 0.41 g; TBHP (70%), 0.45 g; CH_3CN, 6 g; T, 60 °C; t, 12 h; catalyst amount: 0.2 g.
[a] *M*, metal content determined from ICP analysis.
[b] One, cyclohexenone.
[c] TON, turn over number, moles of substrate converted per mole of metal.

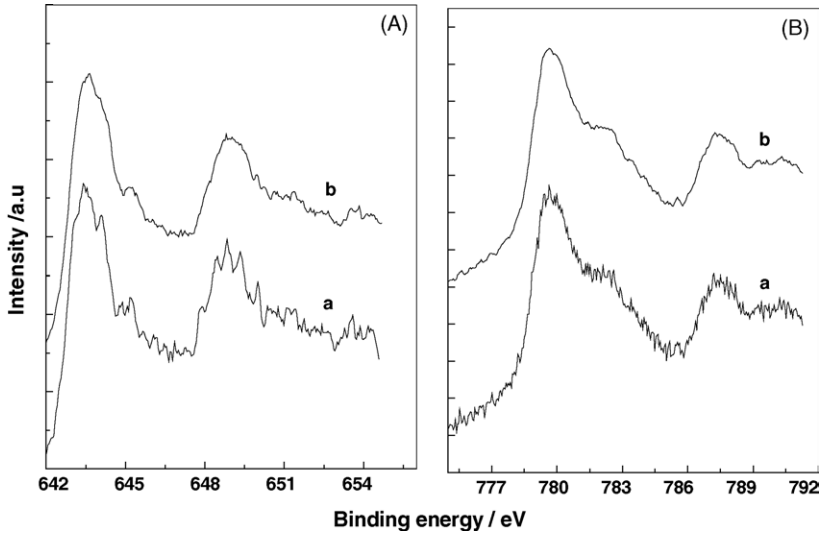

Fig. 6. XPS spectra of: (A) Mn-salen containing mesoporous alumina and (B) Co-salen containing mesoporous alumina, where (a) neat metal complex and (b) immobilized metal complex.

observed with the neat complexes, leading to better activity as well as selectivity to epoxides [25,31]. However, as mentioned earlier, it is inappropriate to compare the catalytic results under neat as well the heterogenized conditions, since the coordination sphere of both complexes is different. Among olefins, styrene conversion is higher than cyclohexene, which may be due to the comparatively easier side chain oxidation than the reactions in the aromatic ring. Interestingly, even though benzaldehyde was the major product obtained during styrene epoxidation, kinetic studies revealed that the formation of phenyl acetaldehyde, an isomerized product of styrene epoxide, is not formed over immobilized catalysts while under neat catalysts, a significant amount of its formation is noted. Hence, it is reasonable to assume that the reaction proceeds under different mechanisms over the homogenous complexes and heterogenous catalysts. Further, in order to ascertain whether the activity of the immobilized catalysts arise from true heterogenous catalysts, the stability of metal complexes were probed by performing typical leaching studies. For that, the catalyst was separated from the reaction mixture after a definite period of time (viz. 2 h) and the hot filtrate was probed for further reactions. Interestingly, it was found that the conversion rate essentially gets terminated after the removal of the catalyst sample, which confirms that the present anchored metal complexes are stable in the reaction medium and are not prone for leaching.

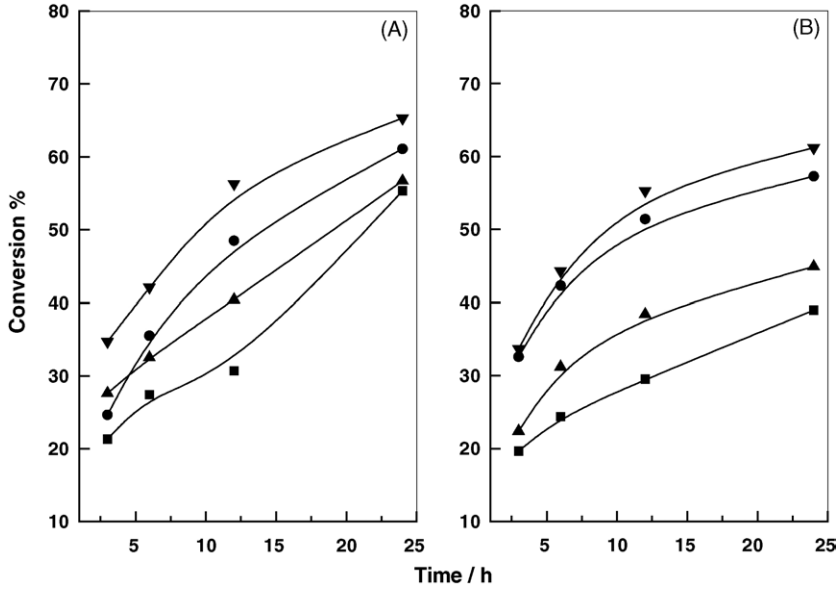

Fig. 7. Reaction kinetic profiles of neat and immobilized Co- and Mn-salen complex in the oxidation reaction of: (A) cyclohexene and (B) styrene, where (■) neat Mn complex; (●) immobilized Mn complex; (▲) neat Co complex; (▼) immobilized Co complex.

Hence, considering the increased stability of the materials, it is reasonable that between the two complex species shown in Scheme 3, complex 1 may be the major species formed. Moreover the catalyst, Mn-S-NH_2-MA, was reused three times in the reaction of styrene without significant differences in the conversion (51.4% changed to 46.4%) and selectivity (27.2% changed to 25.1%) after third run and thereby, relies as novel heterogenous catalysts for various (ep)oxidation reactions.

4. Conclusion

The immobilization of manganese and cobalt complexes over mesoporous alumina, modified previously by 3-APTES, has been achieved by schiff base condensation reaction. Different characterizations techniques, such as XRD, FTIR, TG-DTG, UV–vis and XPS reveal that the complex is attached firmly over the modified alumina surfaces. The molecular dispersion of the complex with sufficient space and hydrophobic surface are appropriate for activation of hydrocarbons as evidenced by the higher TON over immobilized catalysts in the selected epoxidation reactions. Moreover, these new catalysts did not leach its active sites during reactions and are reusable which indicates that the immobilization of neat complexes are effective by the present synthesis protocols over mesoporous alumina.

Acknowledgements

We thank our reviewers for constructive suggestions. The authors are grateful to Dr. N.E. Jacob for adsorption results, Mr. Patel for XPS results and Ms. V. Samuel for XRD results. V.D.C and S.S thanks CSIR, India for senior research fellowships.

References

[1] C.T. Kresge, M.E. Leonowicz, W.J. Roth, J.C. Vartuli, J.S. Beck, Nature 359 (1992) 710.
[2] Q. Huo, D.I. Margolese, V. Ciesla, P. Feng, T.E. Gier, P. Sieger, R. Leon, P.M. Petroff, F. Schuth, G.D. Stucky, Nature 368 (1994) 317.
[3] A. Sayari, P. Liu, Microporous Mater. 12 (1997) 149.
[4] M. Chidambaram, D.C. Ferre, A.P. Singh, B.G. Anderson, J. Catal. 220 (2003) 442.
[5] Y. Iwasawa, Tailored Metal Catalysts, Reidel, Holand, 1986.
[6] A. Kozlov, K. Asakura, Y. Iwasawa, Microporous Mesoporous Mater. 21 (1998) 579.
[7] E.N. Jacobson, W. Zhang, A.R. Muci, J.R. Ecker, L. Deng, J. Am. Chem. Soc. 113 (1991) 7063.
[8] M. Palucki, P.J. Pospisil, W. Zhang, E.N. Jacobson, J. Am. Chem. Soc. 116 (1994) 9333.
[9] R. Irie, K. Noda, Y. Ito, N. Matsumoto, T. Katsuki, Tetrahedron Lett. 31 (1990) 7345.
[10] B.M. Choudary, M.L. Kantam, B. Bharathi, P. Sreekanth, F. Figueras, J. Mol. Catal. A Chem. 159 (2000) 417.
[11] C. Baleizao, B. Cignate, H. Garcia, A. Corma, J. Catal. 215 (2003) 199.
[12] S.R. Cicco, M. Latronico, P. Mastrorilli, G.P. Suranna, C.F. Nobile, J. Mol. Catal. A Chem. 165 (2001) 135.
[13] C. Bowers, P.K. Dutta, J. Catal. 122 (1990) 271.
[14] P.P. Knops-Gerrits, M.L. Abbe, P.A. Jacobs, Stud. Surf. Sci. Catal. 108 (1997) 445.
[15] P.P. Knops-Gerrits, D.E. de Vos, P.A. Jacobs, J. Mol. Catal. 117 (1997) 57.
[16] J. Zhao, J. Han, Y. Zhang, J. Mol. Catal. A Chem. 231 (2005) 129.
[17] K.B.M. Janssen, I. Laquiere, W. Dehaen, R.F. Parton, I.F.J. Vankelecom, P.A. Jacobs, Tetrahedron Asymmetry 8 (1997) 3481.
[18] F. Mintolo, D. Pini, P. Salvadori, Tetrahedron Lett. 37 (1996) 3375.
[19] M.J. Sabater, A. Corma, A. Domenech, V. Fornes, H. Garcia, J. Chem. Soc. Chem. Commun. (1997) 1285.
[20] P. Piaggio, P. McMorn, C. Langham, D. Bethell, P.C. Bulman-Page, F.E. Hancock, G.J. Hutchings, New J. Chem. 22 (1998) 1167.
[21] L. Frunza, H. Kosslick, H. Landmesser, K. Hoft, R. Fricke, J. Mol. Catal. A Chem. 123 (1997) 179.
[22] E.F. Murphy, A. Baiker, J. Mol. Catal. A Chem. 179 (2002) 233.
[23] F. Vaudry, S. Khodabandeh, M.E. Davis, Chem. Mater. 8 (1996) 1451.
[24] M.J. Hudson, J.A. Knowles, J. Mater. Chem. 6 (1996) 89.
[25] S. Shylesh, A.P. Singh, J. Catal. 228 (2004) 333.
[26] S. Shylesh, S. Sharma, S.P. Mirajkar, A.P. Singh, J. Mol. Catal. A Chem. 212 (2004) 219.
[27] P. Karandikar, M. Agashe, K. Vijaymohanam, A.J. Chandwadkar, Appl. Catal. A Gen. 257 (2004) 133.
[28] X.G. Zhou, X.Q. Yu, J.S. Huang, S.G. Li, L.-S. Li, C.M. Che, Chem. Commun. (1999) 1789.
[29] T. Joseph, S.B. Halligudi, C.V.V. Satyanarayana, D.P. Sawant, S. Gopinathan, J. Mol. Catal. A Chem. 168 (2001) 8797.
[30] S.B. Halligudi, K.N. Kalaraj, S.S. Despande, S. Gopinathan, J. Mol. Catal. 154 (2000) 25.
[31] T. Joseph, D.P. Sawant, C.S. Gopinath, S.B. Halligudi, J. Mol. Catal. A Chem. 184 (2002) 289.
[32] D. Briggs, M.P. Seah, Practical Surface Analysis, Auger and X-Ray Photoelectron Spectroscopy, vol. 1, second ed., Wiley, London, 1996, p. 129.
[33] D. Briggs, V.A. Gibson, Chem. Phys. Lett. 25 (1974) 493.
[34] A.R. Silva, J.L. Figueiredo, C. Freire, B.D. Castro, Microporous Mesoporous Mater. 68 (2004) 83.
[35] L. Guezi, R. Sundararajan, Zs. Koppany, Z. Zsoldos, Z. Schay, F. Mizukami, S. Niwa, J. Catal. 167 (1997) 482.